

# Channel-Correlation Adaptive Dictionary Learning based Demosaicking

Chenyan Bai\*, Jia Li<sup>†</sup> and Zhouchen Lin<sup>†</sup>

\*College of Information Engineering

Capital Normal University, Beijing, P.R. China 100048

Email: cybai@cnu.edu.cn

<sup>†</sup>Key Laboratory of Machine Perception (MOE)

School of EECS, Peking University, Beijing, P.R. China 100871

Email: jiali.gm@gmail.com, zlin@pku.edu.cn

**Abstract**—Image demosaicking is the problem of reconstructing color images from raw images captured by a digital camera which is covered by a color filter array (CFA). Sparse representation based demosaicking method achieves excellent performance on the commonly used Kodak PhotoCD dataset. However, it performs inferior on the IMAX dataset. In this paper, we analyze that the factor of the sparse representation based demosaicking methods perform different is channel-correlation. Hence, we propose a channel-correlation adaptive dictionary learning based demosaicking (CADLD). Different from the sparse representation based demosaicking methods that use one fixed dictionary, our method train a general dictionary on training datasets with varies channel-correlations. Then we learn a function matrix between the general dictionary and channel-correlations. For a raw data with a specific channel-correlation, we demosaick it adaptively to its channel-correlation through the function matrix. Experiments confirm the proposed method outperforms other sparse representation based demosaicking methods.

## I. INTRODUCTION

In color digital imaging, color image is reconstructed from raw images captured by a digital camera which is covered by a color filter array (CFA) [1], [2] (Fig. 1). The reconstruction process is called demosaicking. Many demosaicking methods have been developed to improve the quality of the demosaicked images [3]. Among these methods, sparse representation based demosaicking method [4], [5] achieves excellent performance. However, it learns one fixed dictionary to reconstruct the mosaicked images, with the result that the demosaicking effect is not always good when the training and test datasets are in different domains [6]. For example, the learned simultaneous sparse representation (LSSC) method [5] that gets the highest CPSNR on the commonly used Kodak PhotoCD dataset [7] by now. However, it performs inferior on the IMAX dataset [8] which is another popular dataset for demosaicking [6]. Therefore, improving the demosaicking performance on both of the Kodak PhotoCD [7] and IMAX datasets [8] is an important issue.

Recently, researchers point out that channel-correlation [9] is an important factor to make different performances on different datasets. Some interpolation based demosaicking methods [9]–[15] have considered the channel-correlation. For example, Duran [9] proposed an algorithm that introduced a clear manner of balancing how much channel-correlation must

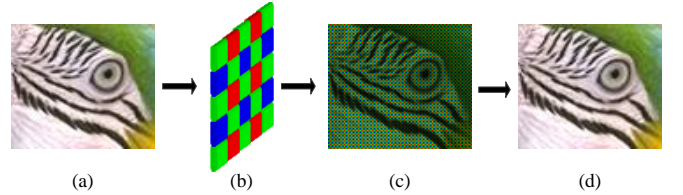


Fig. 1. The process of image demosaicking. (a) A full color image to simulate a real scene. (b) Bayer CFA. (c) Bayer mosaicked image. (d) Bayer demosaicked image. Images in this paper are best viewed on screen!

be taken advantage of. However, their results are not satisfied on both of the two test datasets [6].

In this paper, considering that sparse representation based demosaicking method [4], [5] achieves excellent performance on the Kodak PhotoCD dataset [7] and inferior on the IMAX datasets [8], we first analyze the channel-correlation affect to the performance of the sparse representation based demosaicking methods [4], [5] (see analysis in Section II). Then we propose a channel-correlation adaptive dictionary learning based demosaicking method that can demosaick adaptively to the channel-correlation and perform well in data with different channel-correlations. Different from the sparse representation based demosaicking methods [4], [5] that use one fixed dictionary in test datasets with different channel-correlations, our proposed method train a general dictionary on training datasets with varies channel-correlations. And then we learn a function matrix between the general dictionary and channel-correlations. Finally, for a raw data with a specific channel-correlation, we demosaick it by the sparse representation based method with channel-correlation as its parameter, by which it can demosaick adaptively to the channel-correlation through the function matrix (see the flow chart in Fig 4).

The contributions are as follows:

- We show that channel-correlation is an important factor to affect the performance of the existing sparse representation based demosaicking methods.
- We propose a channel-correlation adaptive dictionary learning based demosaicking method (CADLD) which can demosaick adaptively to data with different channel-correlations.

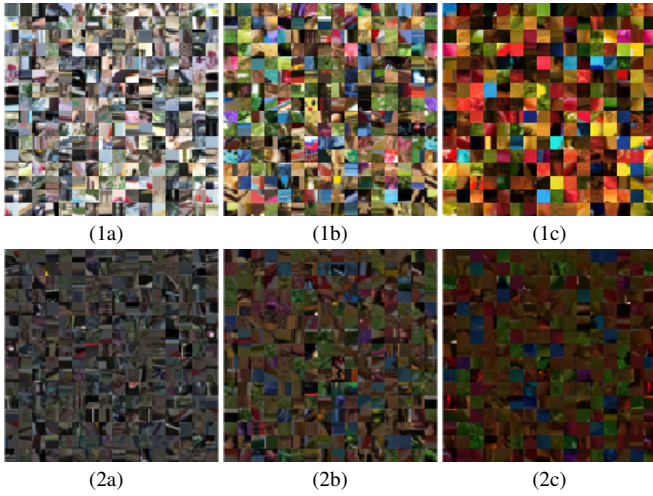


Fig. 2. Illustration of the training data and the corresponding dictionaries with different channel-correlations. (1a), (1b), and (1c) are training patches randomly sampled from the training data with channel-correlations 0.2, 0.5, and 0.8, respectively. (2a), (2b), and (2c) are dictionaries learned on the corresponding training patches.

TABLE I  
SUMMARY OF THE MAIN NOTATIONS USED IN THIS PAPER.

Notation	Definition
$\mathbb{R}$	Set of real numbers
$\mathbf{x}(i)$	$i$ -th element of vector $\mathbf{x}$
$\mathbf{X}(i, j)$	$(i, j)$ -th element of matrix $\mathbf{X}$
$\mathbf{X}^T$	Transpose of matrix $\mathbf{X}$
$\mathbf{X}^\dagger$	Pseudo-inverse of matrix $\mathbf{X}$
$\ \mathbf{x}\ _1$	$\ell_1$ -norm (summation of nonzero elements) of vector $\mathbf{x}$
$\ \mathbf{x}\ _2$	$\ell_2$ -norm $(\sqrt{\sum_i \mathbf{x}(i)^2})$ of vector $\mathbf{x}$
$\ \mathbf{X}\ _F$	Frobenius norm $(\sqrt{\sum_i \sum_j \mathbf{X}(i, j)^2})$ of matrix $\mathbf{X}$

The rest of the paper is organized as follows. In Section II, we introduce the channel-correlation and analyze its effect on the sparse representation based demosaicking. Then we introduce our channel-correlation adaptive dictionary learning based demosaicking method in Section III. In Section IV, we conduct experiments to verify our method. Finally, we conclude the paper in Section V.

## II. ANALYSIS OF CHANNEL-CORRELATION EFFECT ON SPARSE REPRESENTATION BASED DEMOSAICKING

Studies have found that correlations among R, G, and B channels are important factors to affect demosaicking performance [6], [9]. In this section, we analyze the channel-correlation effect on the sparse representation based demosaicking method [5]. The main notations used in the paper are summarized in Table I.

### A. Channel-correlation Effect on Sparse Representation based Demosaicking

We use the channel-correlation defined by [9]. They project the RGB image into the YUV space. Then they define a set of pixels whose luminance gradients are above a threshold, that

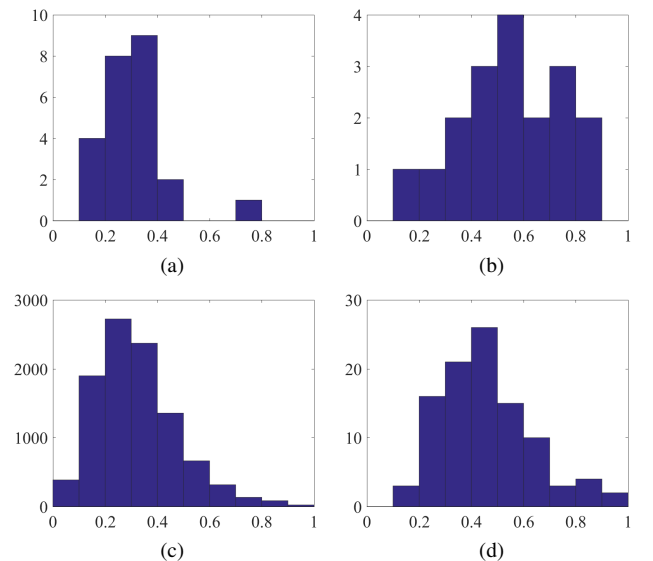


Fig. 3. The channel-correlations' distribution of different test and training datasets computed by (4). (a) and (b) are that of the Kodak PhotoCD [7] and IMAX [8] test datasets. (c) and (d) are that of the PASCAL VOC'07 [16] and DDR [6] training datasets.

is

$$I = \{(i, j) | \Delta Y(i, j) > \theta\}, \quad (1)$$

where  $Y$  is the luminance, and  $\Delta Y$  is the luminance gradient.

Then they compute the  $\ell_1$ -norm of the chromatic gradients on  $I$  as

$$\begin{aligned} \|\Delta U\|_1 &= \frac{1}{2\|I\|_1} \sum_{(i,j) \in I} (|U(i+1, j) - U(i, j)| \\ &\quad + |U(i, j+1) - U(i, j)|), \\ \|\Delta V\|_1 &= \frac{1}{2\|I\|_1} \sum_{(i,j) \in I} (|V(i+1, j) - V(i, j)| \\ &\quad + |V(i, j+1) - V(i, j)|), \end{aligned} \quad (2)$$

where  $\Delta U$  and  $\Delta V$  are the chromatic gradients.

The channel-correlation is defined as the mean value of  $\|\Delta U\|_1$  and  $\|\Delta V\|_1$

$$c = \frac{1}{2}(\|\Delta U\|_1 + \|\Delta V\|_1). \quad (3)$$

We analyze the channel-correlation effect on the sparse representation based demosaicking [5]. We randomly sample patches from the PASCAL VOC'07 [16] and DDR datasets [6] whose channel-correlation distribution histogram are shown in Fig. 3(c) and (d), respectively. We sample  $2 \times 10^6$  patches size of  $8 \times 8 \times 3$  whose channel-correlations are in  $0.2 \pm 0.05$ ,  $0.5 \pm 0.05$ , and  $0.8 \pm 0.05$ , respectively. Then we randomly separate them into  $1.5 \times 10^6$  training (see the first row in Fig. 2) and  $10^6$  test patches.

We directly use the SPAMS toolbox [5], [17] to learn three dictionaries on the three different channel-correlation training datasets. All the dictionaries are of the same size  $192 \times 256$ , which are denoted as  $\mathbf{D}_{0.2}$ ,  $\mathbf{D}_{0.5}$  and  $\mathbf{D}_{0.8}$  (see

TABLE II  
CHANNEL-CORRELATION EFFECT ON SPARSE REPRESENTATION BASED DEMOSAICKING. WE CHOOSE TEST PATCHES WITH THREE CHANNEL-CORRELATIONS 0.2, 0.5, AND 0.8. THEN WE DEMOSAICK THEM BY THREE DICTIONARIES  $\mathbf{D}_{0.2}$ ,  $\mathbf{D}_{0.5}$ , AND  $\mathbf{D}_{0.8}$  LEARNED ON THREE TRAINING PATCHES WITH CHANNEL-CORRELATIONS 0.2, 0.5, AND 0.8, RESPECTIVELY. THE TABLE ILLUSTRATES THE RATIO MATRIX  $\mathbf{R}$  COMPUTED BY (4). IT GETS THE MOST HIGHEST CPSNR (NUMBERS IN BOLD) WHEN THE TEST AND THE TRAINING DATA ARE WITHIN THE SAME CHANNEL-CORRELATION.

Channel-correlation	$\mathbf{D}_{0.2}$	$\mathbf{D}_{0.5}$	$\mathbf{D}_{0.8}$
Test <sub>0.2</sub>	<b>65.50%</b>	28.36%	6.14%
Test <sub>0.5</sub>	21.87%	<b>55.66%</b>	22.46%
Test <sub>0.8</sub>	2.42%	37.24%	<b>60.34%</b>

the second row in Fig. 2). We demosaick the three different channel-correlation test patches by PSRD [18] with dictionaries  $\mathbf{D}_{0.2}$ ,  $\mathbf{D}_{0.5}$  and  $\mathbf{D}_{0.8}$ , respectively.

For each test patch group with the same channel-correlation, we sign on which dictionary it achieve the highest CPSNR. Then we count the number of the highest CPSNR for each dictionary, which is denoted by  $N_h(\mathbf{D}_j)$ ,  $j \in \{0.2, 0.5, 0.8\}$ . For each test patches group with the same channel-correlation  $c$ , we compute the following ratio matrix  $\mathbf{R}$

$$\mathbf{R}(c, j) = \frac{N_h(\mathbf{D}_j)}{N}, \quad (4)$$

where  $N_h(\mathbf{D}_j)$  means the number of the highest CPSNR for dictionary  $\mathbf{D}_j$ , and  $N$  is the total number of the test patches.

The ratio matrix  $\mathbf{R}$  is illustrated in Table II. We can see that the test patches achieve the most highest CPSNR (numbers in bold) demosaicked by the dictionaries learned on the corresponding channel-correlation training patches.

### B. Analysis and Discussions

Specifically, we analyze the channel-correlation effect on LSSC [5] which achieves good performance among the sparse representation based demosaicking methods. We compute the channel-correlation of the training and testing datasets using (4) to analysis its effect on LSSC [5]. The histograms of the Kodak PhotoCD [7] and IMAX dataset [8] are shown in Fig. 3(a) and (b). We can find that the channel-correlations of the Kodak PhotoCD dataset [7] is mainly in (0.2, 0.4), while that of the IMAX dataset [8] is mostly in (0.4, 0.8).

We also compute the channel-correlations of the training dataset of LSSC [5], that is the PASCAL VOC'07 dataset [16]. The histogram is shown in Fig. 3(c). We can find that the channel-correlation distribution of the PASCAL VOC'07 dataset is more similar with that of the Kodak PhotoCD dataset (Fig. 3(a)), which is also mostly in (0.2, 0.4), while is different from that of the IMAX dataset (Fig. 3(b)). So we can get an intuitive explanation of why the LSSC [5] with dictionary learned on the PASCAL VOC'07 dataset achieve excellent performance on the Kodak dataset, while less convincing on the IMAX dataset. This inspire us to develop a channel-correlation adaptive dictionary learning based demosaicking method which we will tell about in Section III.

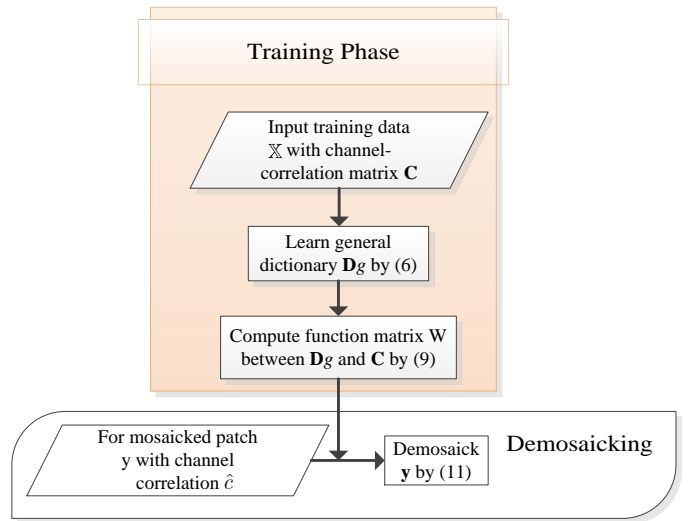


Fig. 4. The flow chart of channel-correlation adaptive dictionary learning based demosaicking. In the training phase, learn a general dictionary  $\mathbf{D}_g$  on training data with different channel-correlations  $\mathbf{C}$  by (6). Then compute the function matrix  $\mathbf{W}$  between  $\mathbf{D}_g$  and  $\mathbf{C}$  (9). In the test phase, demosaick the mosaicked patch  $\mathbf{y}$  by (11).

### III. CHANNEL-CORRELATION ADAPTIVE DICTIONARY LEARNING BASED DEMOSAICKING

We propose a channel-correlation adaptive dictionary learning based demosaicking method which is called CADLD. The CADLD is based on the sparse representation demosaicking [4], [5] and domain adaptive dictionary learning [19]. It can demosaick adaptively to the channel-correlations. The flow chart is shown in Fig 4. It first train a general dictionary on training datasets with different channel-correlations and then learn a function between the general dictionary and channel-correlations. For a test data with a specific channel-correlation, we demosaick it adaptively to its channel-correlation through the function matrix. We give the details bellow.

#### A. Training Phase

Since the sparse representation based demosaicking method [4], [5] cannot work well when the training and test datasets are with different channel-correlations, we develop a channel-correlation adaptive demosaicking method based on dictionary learning and sparse representation.

1) *Learning a General Dictionary:* To deal with the condition when the training and test data are in different domains, Qiu [19] proposed an domain adaptive dictionary learning method in the face recognition problem. It first learns a general dictionary on training face data with different view points. Then for each test face data to be recognized, it estimates the view point of the test data and computes a specific dictionary for it. Finally, the test face data is dealt by the corresponding adaptive dictionary.

Inspired by Qiu [19], we propose a channel-correlation adaptive demosaicking method. We denote  $\mathbf{x} = (\mathbf{x}_R^T, \mathbf{x}_G^T, \mathbf{x}_B^T)^T \in \mathbb{R}^{3m \times 1}$  is a full color image patch, with  $\mathbf{x}_R$ ,  $\mathbf{x}_G$ , and  $\mathbf{x}_B$  being its red, green, and blue

channels, respectively,  $\mathbf{X}_i = (\mathbf{x}_{i1}, \mathbf{x}_{i2}, \dots, \mathbf{x}_{in}) \in \mathbb{R}^{3m \times n}$  is a training dataset consists of  $n$  patches with a specific channel-correlation. Let  $\{\mathbf{X}_i\}_{i=1}^s$  be the training datasets with  $s$  different channel-correlations, we aim to learn dictionaries on these training datasets, which are with the same sparse coefficient matrix  $\mathbf{A} \in \mathbb{R}^{k \times n}$ . The model is as follows

$$\begin{aligned} & \arg \min_{\mathbf{D}_i, \mathbf{A}} \sum_{i=1}^s \|\mathbf{X}_i - \mathbf{D}_i \mathbf{A}\|_F^2 + \lambda \sum_{j=1}^n \|\mathbf{A}(:, j)\|_1 \\ & \text{s.t. } \forall i \|\mathbf{D}_i(:, l)\|_1 = 1, l = 1, 2, \dots, k, \end{aligned} \quad (5)$$

where  $\mathbf{D}_i \in \mathbb{R}^{3m \times k}$  ( $k > 3m$ ) is the dictionary learned on the training data  $\mathbf{X}_i$ .

Let  $\mathbb{X} = (\mathbf{X}_1^T, \mathbf{X}_2^T, \dots, \mathbf{X}_s^T)^T \in \mathbb{R}^{3ms \times n}$  be the whole training data with  $s$  different channel-correlations, through mathematic deduction, (5) can be formulated as

$$\arg \min_{\mathbf{D}_g, \mathbf{A}} \|\mathbb{X} - \mathbf{D}_g \mathbf{A}\|_F^2 + \lambda \sum_{j=1}^n \|\mathbf{A}(:, j)\|_1, \quad (6)$$

where  $\mathbf{D}_g = (\mathbf{D}_1^T, \mathbf{D}_2^T, \dots, \mathbf{D}_s^T)^T$  is the general dictionary. We use SPAMS toolbox [5], [17] to learn the general dictionary. We project  $\mathbf{D}_i$  to satisfy the constraint in (5) for each iteration when update the dictionary.

*2) Learning a Function between Dictionary and Channel-correlation:* Following [19], we model the dictionary as a  $p$  degree polynomial function of the channel-correlation. Let  $\mathbf{d}_i = \text{vec}(\mathbf{D}_i) \in \mathbb{R}^{3mk \times 1}$ , we have

$$\mathbf{d}_i = \mathbf{Wc}_i, \quad (7)$$

where  $\mathbf{W} \in \mathbb{R}^{3mk \times (p+1)}$  is the coefficient matrix of the polynomial function,  $\mathbf{c}_i = (1, c_i, c_i^2, \dots, c_i^p)^T$ .  $p$  is empirically set as 2 in all experiments.

We define  $\mathbf{D}_g^{VT}$  as

$$\begin{aligned} \mathbf{D}_g^{VT} &= (\mathbf{d}_1, \mathbf{d}_2, \dots, \mathbf{d}_s) \\ &= (\mathbf{Wc}_1, \mathbf{Wc}_2, \dots, \mathbf{Wc}_s) \\ &= \mathbf{WC}, \end{aligned} \quad (8)$$

where  $\mathbf{C} = (\mathbf{c}_1, \mathbf{c}_2, \dots, \mathbf{c}_s)$ .

We can compute the function parameter matrix  $\mathbf{W}$  between dictionary and channel-correlation by (8), that is

$$\mathbf{W} = \mathbf{D}_g^{VT} \mathbf{C}^\dagger. \quad (9)$$

### B. Channel-correlation Adaptive Demosaicking

In the noiseless case, the model of color imaging with a CFA is as follows:

$$\mathbf{y} = \mathbf{Mx} = (\mathbf{M}_R, \mathbf{M}_G, \mathbf{M}_B)(\mathbf{x}_R^T, \mathbf{x}_G^T, \mathbf{x}_B^T)^T, \quad (10)$$

where  $\mathbf{y} \in \mathbb{R}^{m \times 1}$  is the raw image patch,  $\mathbf{x} \in \mathbb{R}^{3m \times 1}$  is the color image patch, with  $\mathbf{x}_R$ ,  $\mathbf{x}_G$ , and  $\mathbf{x}_B$  being its red, green, and blue channels, respectively,  $\mathbf{M} \in \mathbb{R}^{m \times 3m}$  is the mosaicking matrix, and  $\mathbf{M}_R$ ,  $\mathbf{M}_G$ , and  $\mathbf{M}_B$  are diagonal matrices whose diagonal elements are specified by the red, green, and blue channels of the CFA, respectively. Formally, let the

TABLE III  
EVALUATION OF THE PROPOSED METHOD ON THE IMAX DATASET [8].  
THE INDIVIDUAL AND AVERAGE CPSNR VALUES ARE REPORTED. “AVG.”  
STANDS FOR “AVERAGE”

Image ID	SC [4]	SSC [5]	LSC [5]	LSSC [5]	PSRD [18]	PAMD [20]	CADLD
01	26.32	26.47	27.58	27.77	26.38	26.31	<b>28.94</b>
02	33.25	33.51	33.68	34.09	33.22	33.07	<b>34.79</b>
03	32.43	32.53	32.79	32.89	32.47	32.42	<b>33.42</b>
04	34.51	34.64	36.18	36.62	34.61	35.25	<b>37.67</b>
05	30.68	30.97	31.47	31.98	30.76	30.54	<b>33.32</b>
06	33.10	34.17	35.13	37.47	33.22	33.91	<b>38.79</b>
07	39.30	39.83	39.04	39.61	39.09	<b>40.16</b>	39.06
08	37.80	38.28	38.09	38.79	37.80	37.31	<b>38.99</b>
09	34.97	35.42	35.81	36.46	34.97	34.36	<b>37.54</b>
10	36.42	36.96	36.98	37.92	36.33	36.24	<b>38.70</b>
11	37.20	38.01	37.93	39.21	37.07	37.24	<b>39.87</b>
12	36.58	36.83	37.13	37.68	36.49	36.08	<b>38.83</b>
13	38.60	39.03	38.99	39.72	38.41	38.38	<b>40.64</b>
14	36.74	37.28	37.29	38.00	36.67	36.60	<b>38.76</b>
15	37.23	37.74	37.59	38.43	37.13	36.94	<b>39.12</b>
16	29.48	29.69	31.12	31.63	29.60	29.53	<b>33.57</b>
17	29.46	29.83	31.04	31.84	29.53	29.61	<b>33.47</b>
18	33.56	33.65	34.02	34.60	33.56	33.46	<b>35.49</b>
Avg.	34.31	34.71	35.10	35.82	34.29	34.30	<b>36.72</b>

CFA be  $\mathbf{C} \in \mathbb{R}^{\sqrt{m} \times \sqrt{m} \times 3}$ , then  $\mathbf{M}_R = \text{Diag}(\text{vec}(\mathbf{C}(:, :, 1)))$ ,  $\mathbf{M}_G = \text{Diag}(\text{vec}(\mathbf{C}(:, :, 2)))$ , and  $\mathbf{M}_B = \text{Diag}(\text{vec}(\mathbf{C}(:, :, 3)))$ .

For a raw data  $\mathbf{y}$  with channel-correlation  $\hat{c}$ , we propose the following adaptive demosaicking model

$$\min_{\mathbf{y}, \boldsymbol{\alpha}} \frac{1}{2} \|\mathbf{y} - \mathbf{MW}\hat{c}\boldsymbol{\alpha}\|_2^2 + \lambda \|\boldsymbol{\alpha}\|_1, \quad (11)$$

where  $\mathbf{M}$  is the mosaicking matrix,  $\mathbf{W}$  is the function parameter matrix between dictionary and channel-correlation, which is computed by (8),  $\hat{c} = (1, \hat{c}, \hat{c}^2, \dots, \hat{c}^p)^T$  is the channel-correlation vector, and  $\boldsymbol{\alpha}$  is the sparse coefficient.

For test patches to be demosaicked, we use the Matlab’s `demosaic` function to demosaick the test patches. Then we estimate their channel-correlations  $\hat{c}$  by the demosaicked color patches.

## IV. EXPERIMENTS

In this section, we conduct our CADLD on the most commonly used datasets. We first give the experimental settings. Then we choose the most latest demosaicking methods and compare our method with them.

### A. Experimental Settings

In the experiments, we sample training patches and learn a function parameter between dictionary and channel-correlation. Then for an arbitrary test patch, we estimate its channel-correlation and demosaick it adaptively using sparse representation based method.

*1) Training Datasets:* We randomly sample patches from two datasets: the PASCAL VOC’07 dataset [16] and the DDR dataset [6]. We sample patches whose channel-correlations are in  $0.2 \pm 0.05$ ,  $0.5 \pm 0.05$ , and  $0.8 \pm 0.05$ , respectively. The sampled number is  $2 \times 10^6$  for each of the channel-correlation, and the patch size is  $8 \times 8 \times 3$ .

TABLE IV

EVALUATION OF THE PROPOSED METHOD ON THE KODAK DATASET [7]. THE INDIVIDUAL AND AVERAGE CPSNR VALUES ARE REPORTED. “AVG.” STANDS FOR “AVERAGE”. WE CAN SEE THAT OUR CADLD IS THE SECOND ONLY TO LSSC [5]

Image ID	SC [4]	SSC [5]	LSC [5]	LSSC [5]	PSRD [18]	PAMD [20]	CADLD
01	40.85	41.33	40.93	41.38	40.51	<b>41.74</b>	40.87
02	41.75	41.95	42.01	<b>42.19</b>	41.90	41.58	42.14
03	43.20	43.40	43.94	<b>44.21</b>	43.20	43.10	44.02
04	42.24	42.47	42.45	<b>42.81</b>	42.20	41.09	42.58
05	38.79	38.96	39.22	<b>39.46</b>	38.88	38.20	38.94
06	41.34	41.69	41.41	<b>41.74</b>	41.20	41.57	41.55
07	43.26	43.56	43.55	<b>43.96</b>	43.30	42.68	43.67
08	37.47	37.60	37.43	37.58	37.44	<b>37.64</b>	37.20
09	43.21	43.42	43.73	<b>43.91</b>	43.13	43.16	43.70
10	42.89	42.99	43.07	<b>43.24</b>	42.82	42.65	43.17
11	41.25	41.40	41.34	<b>41.55</b>	41.22	40.85	41.30
12	44.28	44.62	44.47	<b>44.88</b>	44.26	44.44	44.62
13	36.21	36.36	36.34	<b>36.47</b>	36.00	37.13	36.39
14	37.78	37.95	38.61	<b>38.83</b>	37.93	36.87	38.02
15	41.03	41.45	41.23	<b>41.76</b>	41.00	40.38	41.41
16	44.36	44.84	44.42	<b>44.90</b>	44.35	44.72	44.80
17	41.81	41.94	41.86	42.02	41.80	41.94	<b>42.03</b>
18	38.13	38.23	38.30	<b>38.46</b>	38.07	37.90	38.37
19	41.86	42.10	42.02	<b>42.34</b>	41.65	41.49	42.17
20	41.92	41.96	42.21	<b>42.19</b>	41.75	41.72	42.06
21	40.60	40.68	40.64	<b>40.70</b>	40.47	40.94	40.52
22	38.81	39.03	39.04	<b>39.33</b>	38.83	38.64	39.10
23	43.47	43.79	43.93	<b>44.27</b>	43.48	43.10	44.16
24	35.53	35.53	35.77	<b>35.81</b>	35.50	35.58	35.64
Avg.	40.92	41.14	41.16	<b>41.42</b>	40.87	40.80	41.18

TABLE V

AVERAGE EVALUATION OF THE PROPOSED METHOD ON THE KODAK [7] AND IMAX DATASET [8]. THE AVERAGE CPSNR VALUES ON BOTH OF THE TWO DATASETS ARE REPORTED. “AVG.” STANDS FOR “AVERAGE”

Dataset	SC [4]	SSC [5]	LSC [5]	LSSC [5]	PSRD [18]	PAMD [20]	CADLD
IMAX	34.31	34.71	35.10	35.82	34.29	34.30	<b>36.72</b>
Kodak	40.92	41.14	41.16	<b>41.42</b>	40.87	40.80	41.18
Avg.	37.62	37.93	38.13	38.62	37.58	37.55	<b>38.95</b>

2) *Compared Methods:* We compare our CADLD with the latest sparse representation based demosaicking methods. They are SC [4], SSC [5], LSC [5], LSSC [5], PSRD [18], and PAMD [20].

### B. Results

We conduct experiments on the the IMAX [8] and Kodak PhotoCD dataset [7], respectively. We compare the experimental results by CPSNR and subjective quality. The CPSNR on the IMAX dataset [8] is shown in Table III. We can see that our CADLD outperforms other demosaicking methods on both individual image and the whole dataset. The results on Kodak PhotoCD dataset [7] is shown in Table IV. We can see that our CADLD is the second only to LSSC [5]. Finally, we give the average results on both the two test datasets are shown in Table V. We can see that our CADLD get the highest average CPSNR on the two datasets.

As the visual quality is typically an important evaluation for image demosaicking, we present part of the visual comparison in Fig. 5 and 6. We can see that the visual quality of CADLD is better than that of other demosaicking methods, especially

in well reconstructing along edges (see Fig. 5) and removing false color at highly textured regions (see Fig. 6) (Please read detail descriptions on visual difference in the captions.)

### V. CONCLUSIONS AND FUTURE WORK

In this paper, we propose a channel-correlation adaptive dictionary learning based demosaicking method which can get good performance on test datasets with varies channel-correlations. In the future, we want to define a channel-correlation which can reflect image character better and try to improve the results significantly.

### ACKNOWLEDGMENT

The authors would like to thank the support of the Key Laboratory of Machine Perception (Ministry of Education), Youth Innovative Research Team of Capital Normal University, and the NVIDIA Corporation.

### REFERENCES

- [1] C. Bai, J. Li, Z. Lin, and J. Yu, “Automatic design of color filter arrays in the frequency domain,” *IEEE Transactions on Image Processing*, vol. 25, no. 4, pp. 1793–1807, 2016.
- [2] J. Li, C. Bai, Z. Lin, and J. Yu, “Automatic design of high-sensitivity color filter arrays with panchromatic pixels,” *IEEE Transactions on Image Processing*, vol. 26, no. 2, pp. 870–883, 2017.
- [3] C. Bai, J. Li, Z. Lin, J. Yu, and Y.-W. Chen, “Penrose demosaicking,” *IEEE Transactions on Image Processing*, vol. 24, no. 5, pp. 1672–1684, 2015.
- [4] J. Mairal, M. Elad, and G. Sapiro, “Sparse representation for color image restoration,” *IEEE Transactions on Image Processing*, vol. 17, no. 1, pp. 53–69, 2008.
- [5] J. Mairal, F. Bach, J. Ponce, G. Sapiro, and A. Zisserman, “Non-local sparse models for image restoration,” in *Proceedings of IEEE International Conference on Computer Vision*. IEEE, 2009, pp. 2272–2279.
- [6] J. Wu, R. Timofte, and G. L. Van, “Demosaicing based on directional difference regression and efficient regression priors,” *IEEE Transactions on Image Processing*, vol. 25, no. 8, pp. 3862–3874, 2016.
- [7] “Kodak Lossless True Color Image Suite,” <http://r0k.us/graphics/kodak/>, December 1, 2013.
- [8] “IMAX Dataset,” [http://www4.comp.polyu.edu.hk/~cslzhang/CDM\\_Dataset.htm](http://www4.comp.polyu.edu.hk/~cslzhang/CDM_Dataset.htm), April 1, 2010.
- [9] J. Duran and A. Buades, “Self-similarity and spectral correlation adaptive algorithm for color demosaicking,” *IEEE Transactions on Image Processing*, vol. 23, no. 9, pp. 4031–4040, 2014.
- [10] L. Zhang and X. Wu, “Color demosaicking via directional linear minimum mean square-error estimation,” *IEEE Transactions on Image Processing*, vol. 14, no. 12, pp. 2167–2178, 2005.
- [11] D. Palij, V. Katkovnik, R. Bilcu, S. Alenius, and K. Egiazarian, “Spatially adaptive color filter array interpolation for noiseless and noisy data,” *International Journal of Imaging Systems and Technology*, vol. 17, no. 3, pp. 105–122, 2007.
- [12] I. Pekkucuksen and Y. Altunbasak, “Multiscale gradients-based color filter array interpolation,” *IEEE Transactions on Image Processing*, vol. 22, no. 1, pp. 157–165, 2013.
- [13] ———, “Gradient based threshold free color filter array interpolation,” in *the 17th IEEE International Conference on Image Processing*. IEEE, 2010, pp. 137–140.
- [14] D. Kiku, Y. Monno, M. Tanaka, and M. Okutomi, “Minimized-Laplacian residual interpolation for color image demosaicking,” in *IS&T/SPIE Electronic Imaging*. International Society for Optics and Photonics, 2014, pp. 90 230L–90 230L.
- [15] L. Zhang, X. Wu, A. Buades, and X. Li, “Color demosaicking by local directional interpolation and nonlocal adaptive thresholding,” *Journal of Electronic Imaging*, vol. 20, no. 2, pp. 016–023, 2011.
- [16] Everingham, M. and Van Gool, L. and Williams, C. K. I. and Winn, J. and Zisserman, A., “The PASCAL Visual Object Classes Challenge 2007 (VOC2007) Results,” <http://www.pascal-network.org/challenges/VOC/voc2007/workshop/index.html>, February 9, 2017.

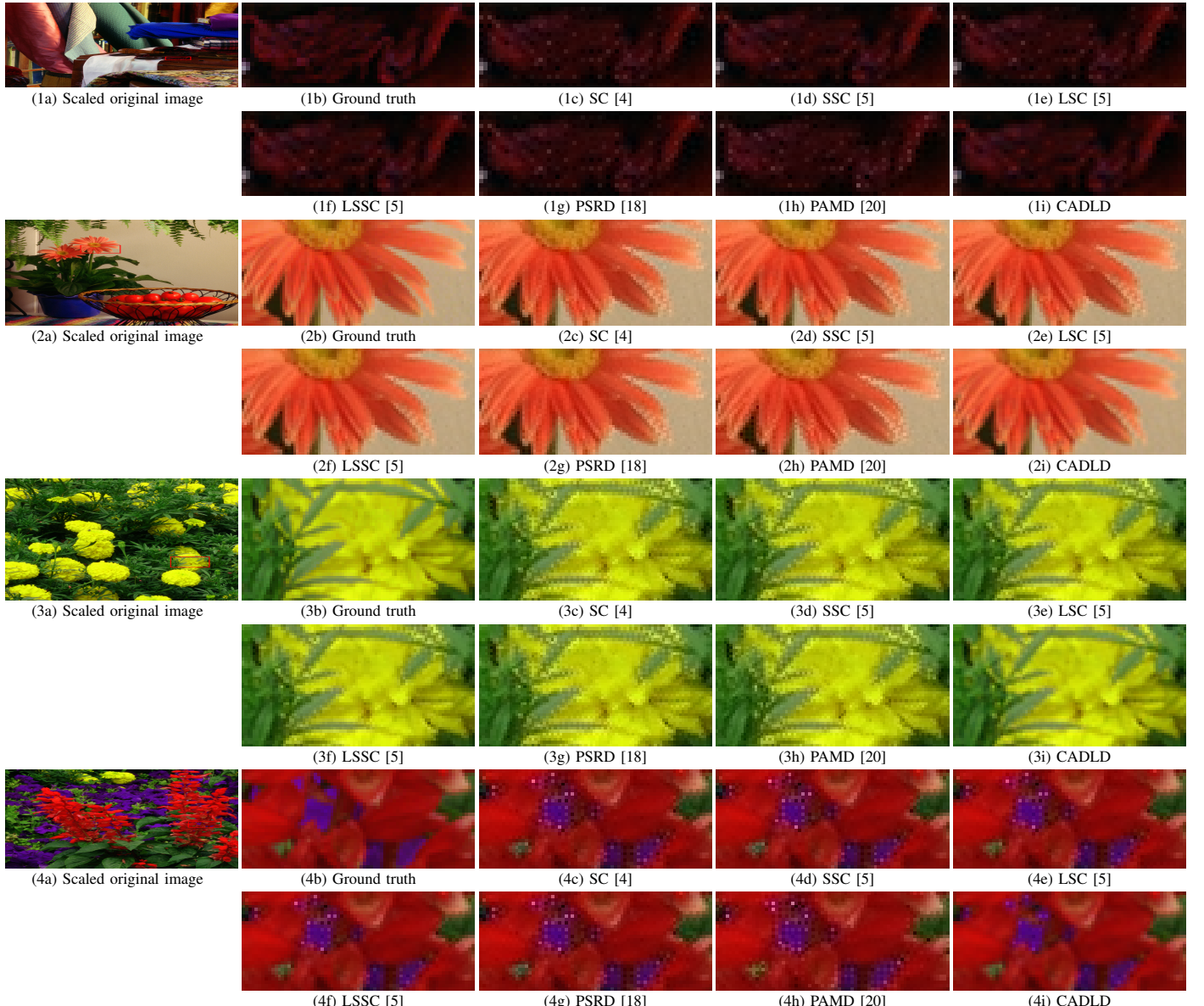


Fig. 5. Blowups of some demosaicked images in the IMAX dataset. From top to bottom, the images are from #2, #9, #16, and #17 images of the IMAX dataset, respectively. In each group, (a) is the scaled original image, in which the red rectangle indicates the selected patch to blow up; (b) is the ground truth; (c)-(h) are the images demosaicked by other dictionary learning methods; (i) are the images demosaicked by our CADLD. From all the four groups of images, we can clearly see that the images demosaicked by others have severe zipper effect, while those by our CADLD have better subjective quality.

- [17] “SPArse Modeling Software,” <http://spams-devel.gforge.inria.fr/>, May 10, 2016.
- [18] J. Li, C. Bai, Z. Lin, and J. Yu, “Optimized color filter arrays for sparse representation based demosaicking,” *IEEE Transactions on Image Processing*, vol. 26, no. 5, pp. 2381–2393, 2017.
- [19] Q. Qiu, V. M. Patel, P. Turaga, and R. Chellappa, “Domain adaptive dic-
- tionary learning,” in *Proceedings of European Conference on Computer Vision*, 2012, pp. 631–645.
- [20] M. Zhang and L. Tao, “A patch aware multiple dictionary framework for demosaicing,” in *Asian Conference on Computer Vision*, 2014, pp. 236–251.

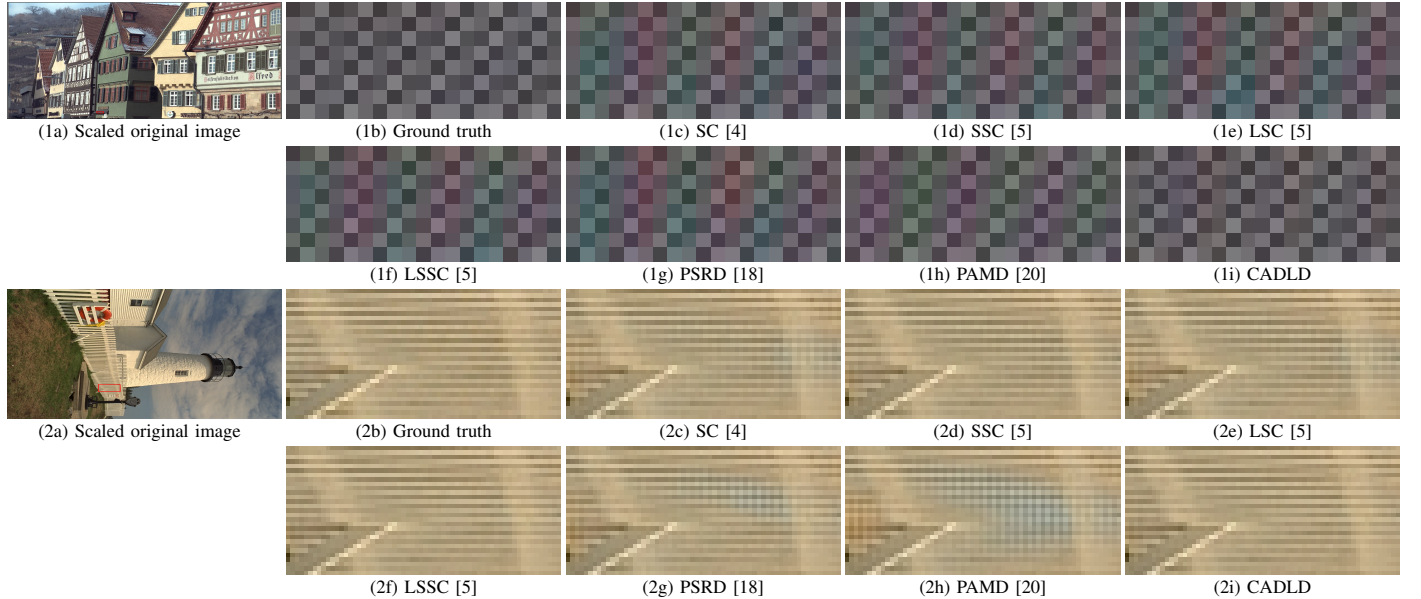


Fig. 6. Blowups of some demosaicked images in the Kodak dataset. From top to bottom, the images are from #8 and #19 images of the Kodak dataset, respectively. In each group, (a) is the scaled original image, in which the red rectangle indicates the selected patch to blow up; (b) is the ground truth; (c)-(h) are the images demosaicked by other dictionary learning methods; (i) are the images demosaicked by our CADLD. From all the four groups of images, we can clearly see that the images demosaicked by others have severe false color (the first group and (2g)-(2h)) or zipper effect ((2c)-(2f) of the second group), while those by our CADLD have better subjective quality.